ISSN 1063-7850, Technical Physics Letters, 2017, Vol. 43, No. 3, pp. 254–257. © Pleiades Publishing, Ltd., 2017.
Original Russian Text © R.V. Gorev, V.L. Mironov, 2017, published in Pis'ma v Zhurnal Tekhnicheskoi Fiziki, 2017, Vol. 43, No. 5, pp. 46–52.

Ferromagnetic Resonance of a Magnetostatically Stabilized Domain Wall in a Nanowire–Nanoparticle Planar System

R. V. Gorev and V. L. Mironov*

Institute for Physics of Microstructures, Russian Academy of Sciences, Nizhny Novgorod, 603087 Russia

**e-mail: mironov@ipmras.ru*

Received July 15, 2016

Abstract—The results of micromagnetic simulation of induced high-frequency magnetization oscillations in a planar ferromagnetic system composed of a magnetostatically coupled nanowire and nanoparticle are reported. The possibility of transformation of the spectrum of this system by introducing a domain wall stabilized with the magnetic field of the nanoparticle into the nanowire is discussed. The dependences of the frequency and amplitude of resonant oscillations of the domain wall on the geometric parameters of the system are analyzed.

DOI: 10.1134/S1063785017030075

Recently, much attention has been paid to ferromagnetic resonance (FMR) of domain walls (DWs) in thin-film ferromagnetic structures [1–4] because of their possible application in microwave electronics devices based on planar waveguides [5–7]. The model objects for this field of research are ferromagnetic nanowires with isolated DWs, resonant oscillations in which are excited by a spin-polarized current or external magnetic field [8–11]. The DW resonance characteristics depend strongly on the geometric parameters of nanowires and the means of DW pinning.

Various versions of traps can be applied to stabilize the DW position in a nanowire. The simplest means of DW pinning are implemented by changing the nanowire shape (narrowing, expansion, thinning, or thickening) in the vicinity of the trap [12–16] are more promising traps based on the magnetostatic interaction of a DW with local stray magnetic fields of the systems of single-domain nanoparticles located near the nanowire [17–22]. In this case, one can change the DW potential-energy profile by changing the spatial position and magnetic state of nanoparticle systems [19–22] and, thus, vary the microwave properties of nanowires with DW in a fairly wide range.

This Letter is devoted to micromagnetic simulation of high-frequency magnetization oscillations in a planar system composed of a nanowire and a single-domain nanoparticle. Particular attention is paid to the resonance related to the DW. From the experimental point of view, the interest in this system is caused by new possibilities of detecting local FMR by the methods of magnetic resonance force microscopy [23–25].

In this study, we investigated ferromagnetic resonance in a planar system composed of a nanowire and a nanoparticle oriented perpendicular to the nanowire axis. The lateral sizes of the nanowire and nanoparticle were 1000×100 and 300×100 nm, respectively. Gap d between the nanoparticle and nanowire was 60 nm. Since the type of DW depends strongly on the nanowire thickness [26], the calculations were performed for two thicknesses: 20 nm (transverse domain wall) and 40 nm (vortex domain wall).

The spatial distributions of magnetization and ferromagnetic resonance were simulated based on numerical solution of the Landau–Lifshitz–Gilbert equation for sample magnetization using the Object Oriented MicroMagnetic Framework (OOMMF) program package [27]. The calculations were performed for a system made of Permalloy ($Ni_{80}Fe_{20}$) with the following parameters: saturation magnetization 8×10^5 A/m, exchange constant 1.3×10^{-11} J/m, and dissipation parameter 0.01 (crystallographic anisotropy was not taken into account). In the simulation, the system was initially brought to the equilibrium state, after which an ac magnetic field was applied to it along the nanowire, and the amplitude of steady-state oscillations was recorded. Frequency ν of the excitation microwave field changed in the range from 0 to 14 GHz with a step of 0.1 GHz. There was no external dc magnetic field. To analyze the oscillation spectra, we plotted the frequency dependences of the

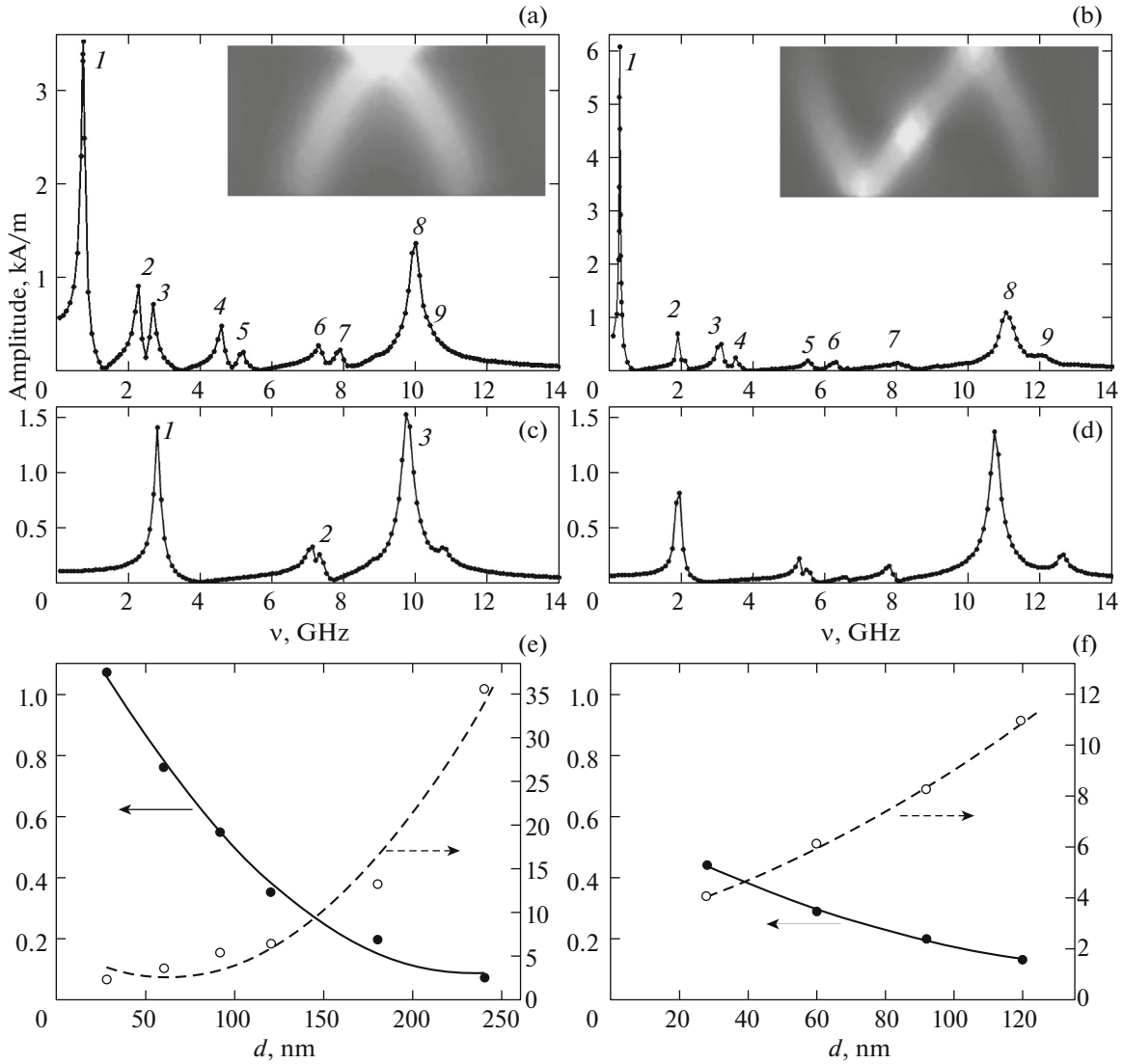

Fig. 1. (a–d) Magnetization oscillation spectra of the nanowire–nanoparticle system: (a) thickness $d = 20$ nm, with transverse DW; (b) $d = 40$ nm, with vortex DW; (c) $d = 20$ nm, without DW; and (d) $d = 40$ nm, without DW. The spatial distributions of the oscillation amplitude at the fundamental DW resonance are shown in the insets. (e, f) Dependences of the resonant DW frequency (closed circles, in GHz) and the resonance amplitude (open circles, in kA/m) on the nanowire–nanoparticle distance: (e) $d = 20$ nm, transverse DW; and (f) $d = 40$ nm, vortex DW.

average-over-system amplitude of oscillations of the magnetization variable component

$$|\mathbf{m}| = \sqrt{m_x^2 + m_y^2 + m_z^2}.$$

To analyze the mode composition of the resonances, we calculated time realizations of the spatial distributions of the amplitude of oscillations of the magnetization variable component under pumping at the resonant frequencies [28, 29].

The FMR in the nanowire–nanoparticle planar system (20 nm thick) with a transverse DW was investigated at the first stage. This state was formed by magnetizing the system in a uniform magnetic field directed along the major axis of the nanoparticle. After switching off the field, the nanowire was relaxed into the state with a transverse DW. The spectrum of magnetization induced oscillations for this case is shown in Fig. 1a. This spectrum contains a number of peaks corresponding to the coupled resonant oscillations of magnetization of the nanowire and nanoparticle. Analysis of the spatial distributions shows that peaks *1*, *2*, *5*, and *9* are caused by the magnetization resonances in the nanowire, whereas peaks *3*, *4*, *6*, *7*, and *8* are caused by the resonances in the nanoparticle. The strong resonance at a frequency of 0.76 GHz is due to the localized DW resonant oscillations. The spatial distribution of the intensity of this oscillation mode is

shown in the inset in Fig. 1a. The oscillation maximum is implemented near the nanowire edge.

In the second stage, we investigated the FMR in the nanowire–nanoparticle system (20 nm thick) without a DW. This state was formed by magnetization along the nanowire axis. The oscillation spectrum for this case is shown in Fig. 1c. Analysis of the corresponding spatial distributions shows that strong peaks *1–3* in this case are caused by only resonances in the nanoparticle. No resonances are excited in the nanowire during such pumping.

The intensity and position of the resonance caused by the transverse DW can be varied in a fairly wide range by changing the gap between the nanoparticle and nanowire (Fig. 1e). At distances $d > 250$ nm, the transverse DW is not retained by the nanoparticle field any longer and leaves the nanowire.

At the third stage, we investigated the FMR in the nanowire–nanoparticle system (40 nm thick) with a vortex DW. The states with the DW and without it were formed in a similar way. The oscillation spectrum of this system is shown in Fig. 1b. In this case, peaks *1*, *3*, and *9* are caused by the magnetization resonances in the nanowire, whereas peaks *2*, *4*, *7*, and *8* are caused by the resonances in the nanoparticle. The fundamental DW resonance (peak *1*) is observed at a frequency of 0.3 GHz. The significant increase in the intensity of this resonant peak (in comparison with the transverse-DW resonance) is likely due to an increase in the volume of the DW region. The spatial distribution of the resonance amplitude for this case (Fig. 1b, inset) shows that three nanowire regions participate in this oscillation. One region is related to the vortex center, while the two others are due to the portions near the nanowire edge with magnetization resembling transverse DWs on the left and right from the vortex. When the system is magnetized along the nanowire axis, the vortex DW leaves the nanowire and, correspondingly, the strong peak caused by DW oscillations disappears (Fig. 1d).

The intensity and position of the resonant peak of the vortex DW can also be varied in a wide range by changing the gap between the nanoparticle and nanowire (Fig. 1f). At distances $d > 130$ nm, the vortex DW is not retained by the nanoparticle field anymore and leaves the nanowire.

We presented the results of micromagnetic simulation of induced magnetization oscillations in nanowire–nanoparticle planar systems with domain walls of two types: transverse for the systems 20 nm thick and vortex for the system 40 nm thick. It was shown that the presence of DW induces strong resonant peaks in the frequency range of 0.1–1 GHz in the oscillation spectrum, which are related to localized DW magnetization oscillations. The intensity and position of these resonant peaks can be varied in a wide range by changing the gap between the nanoparticle and nanowire. The longitudinal magnetization reversal of the nanowire leads to elimination of the DW and, accordingly, the absence of absorption in this frequency range. From the practical point of view, such structures can be applied as switchable elements in microwave electronics devices based on planar waveguides.

Acknowledgments. We are grateful to E.V. Skorokhodov, M.V. Sapozhnikov, and A.A. Fraerman for helpful discussions. This study was supported by the Russian Science Foundation, project no. 16-02-10254.

REFERENCES

1. G. M. Moore, R. L. Stamps, and R. Street, IEEE Trans. Magn. **35**, 3790 (1999).
2. S. D. Mal'ginova, R. A. Doroshenko, and N. V. Shul'ga, J. Magn. Magn. Mater. **296**, 13 (2006).
3. N. Vukadinovic, M. Labrune, J. Ben Youssef, et al., Phys. Rev. B **65**, 054403 (2001).
4. N. Vukadinovic, J. Ben Youssef, N. Beaulieu, and V. Castel, Phys. Rev. B **92**, 214408 (2015).
5. H. Zhang, A. Hoffmann, R. Divan, and P. Wang, Appl. Phys. Lett. **95**, 232503 (2009).
6. J. Ding, M. Kostylev, and A. O. Adeyeye, Phys. Rev. Lett. **107**, 047205 (2011).
7. J. Ding and A. O. Adeyeye, Appl. Phys. Lett. **101**, 103117 (2012).
8. E. Saitoh, H. Miyajima, T. Yamaoka, and G. Tatara, Nature **432**, 203 (2004).
9. A. T. Galkiewicz, L. O'Brien, P. S. Keatley, et al., Phys. Rev. B **90**, 024420 (2014).
10. L. O'Brien, E. R. Lewis, A. Fernandez-Pacheco, et al., Phys. Rev. Lett. **108**, 187202 (2010).
11. P. S. Keatley, W. Yu, and L. O'Brien, J. Appl. Phys. **115**, 17D507 (2014).
12. E. R. Lewis, D. Petit, L. Thevenard, et al., Appl. Phys. Lett. **95**, 152505 (2009).
13. D. Petit, A. V. Jausovec, D. E. Read, and R. P. Cowburn, J. Appl. Phys. **103**, 114307 (2008).
14. D. Petit, A. V. Jausovec, H. T. Zeng, et al., Phys. Rev. B **79**, 214405 (2009).
15. K. O'Shea, S. McVitie, J. N. Chapman, and J. M. R. Weaver, Appl. Phys. Lett. **93**, 202505 (2008).
16. L. K. Bogart, D. Atkinson, K. O'Shea, et al., Phys. Rev. B **79**, 054414 (2009).
17. L. O'Brien, D. Petit, E. R. Lewis, et al., Phys. Rev. Lett. **106**, 087204 (2011).
18. S. M. Ahn, K. W. Moon, C. G. Cho, and S. B. Choe, Nanotecnology **22**, 085201 (2011).
19. V. L. Mironov, O. L. Ermolaeva, E. V. Skorohodov, and A. Yu. Klimov, Phys. Rev. B **85**, 144418 (2012).
20. V. L. Mironov and O. L. Ermolaeva, Bull. Russ. Acad. Sci.: Phys. **78**, 16 (2014).
21. O. L. Ermolaeva, E. V. Skorokhodov, and V. L. Mironov, Phys. Solid State **58**, 2223 (2016).
22. V. L. Mironov, O. L. Ermolaeva, and E. V. Skorohodov, IEEE Trans. Magn. **52**, 1100607 (2016).

23. O. Klein, G. de Loubens, V. V. Naletov, et al., Phys. Rev. B **78**, 144410 (2008).
24. B. Pigeau, C. Hahn, G. de Loubens, et al., Phys. Rev. Lett. **109**, 247602 (2012).
25. I. Lee, Yu. Obukhov, G. Xiang, et al., Nature **466**, 845 (2010).
26. M. Kläui, J. Phys.: Condens. Matter **20**, 313001 (2008).
27. M. J. Donahue and D. G. Porter, *OOMMF User's Guide*, Interagency Rep. NISTIR 6376 (Natl. Inst. Standards Technol., Gaithersburg, 2006). http://math.nist.gov/oommf.
28. R. V. Gorev, V. L. Mironov, and E. V. Skorokhodov, J. Surf. Invest.: X-ray, Synchrotron Neutron Tech. **10**, 298 (2016).
29. R. V. Gorev, E. V. Skorokhodov, and V. L. Mironov, Phys. Solid State **58**, 2212 (2016).

Translated by A. Sin'kov